Loss of NSUN6 inhibits osteosarcoma progression by downregulating EEF1A2 expression and activation of Akt/mTOR signaling pathway via m⁵C methylation

SANG HU[1*], MIN YANG[2*], KANGWEN XIAO[1], ZHIQIANG YANG[1], LIN CAI[1], YUANLONG XIE[1], LINLONG WANG[1] and RENXIONG WEI[1]

[1]Department of Spine Surgery and Musculoskeletal Tumor, Zhongnan Hospital of Wuhan University, Wuhan, Hubei 430071;
[2]Department of Orthopedics, Jingzhou Hospital Affiliated to Yangtze University, Jingzhou, Hubei 434020, P.R. China

Abstract. As an important 5-methylcytidine (m⁵C) methyltransferase, NOP2/Sun RNA methyltransferase family member 6 (NSUN6) has been reported to play an important role in the progression of several diseases. However, the role of NSUN6 in the progression of osteosarcoma (OS) remains unclear. This study aimed to identify the role of NSUN6 in the progression of OS and clarify the potential molecular mechanism. The present study discovered that NSUN6 was upregulated in OS and a higher NSUN6 expression was a strong indicator for poorer prognosis of patients with OS. In addition, the loss of NSUN6 led to reduced proliferation, migration and invasion of OS cells. Through bioinformatics analysis, RNA immunoprecipitation (RIP) and methylated RIP assays, eukaryotic elongation factor 1 α-2 (EEF1A2) was identified and validated as a potential target of NSUN6 in OS. Mechanistically, the expression of EEF1A2 was significantly suppressed following NSUN6 knockdown due to reduced EEF1A2 mRNA stability in an m⁵C-dependent manner. Meanwhile, NSUN6 deficiency inhibited m⁵C-dependent activation of Akt/mTOR signaling pathway. In addition, genetic overexpression of EEF1A2 or pharmacological activation of the Akt signaling pathway counteracted the suppressive effects of NSUN6 deficiency on the proliferation, invasion and migration of OS cells.

Correspondence to: Professor Linlong Wang or Professor Renxiong Wei, Department of Spine Surgery and Musculoskeletal Tumor, Zhongnan Hospital of Wuhan University, 169 Donghu Road, Wuhan, Hubei 430071, P.R. China
E-mail: every24@163.com
E-mail: renxiong.wei@whu.edu.cn

*Contributed equally

The current findings suggested that NSUN6 may serve as a potential therapeutic target for OS treatment.

Introduction

As one of the most prevalent primary malignant bone tumors, osteosarcoma (OS) commonly occurs in adolescents, children and elderly individuals (>60 years old), and is characterized by rapid lung metastasis (1,2). It was reported that the 5-year survival rate of patients with OS without lung metastasis is <70%, while the survival rate reduces significantly to <30% with lung metastasis (3,4). At present, the first-line treatment strategy for OS is surgical excision combined with chemotherapy. However, it becomes increasingly more challenging to manage OS due to the development of chemotherapy resistance and tumor relapse (5-7). Therefore, it is crucial to explore the molecular mechanism that governs lung metastasis, relapse and drug resistance of OS. Recent studies found that autophagy and ferroptosis are involved in the progression and chemotherapy resistance of OS (8-11).

Substantial evidence demonstrated that epigenetics, such as RNA methylation, play vital role in the pathogenesis of various cancers (12-14). Based on methylation sites, RNA methylation can be divided into several types, such as N6-methyladenosine (m6A), 5-methylcytidine (m⁵C), N1-methyladenosine, 2'-O-methylation, 3-methylcytidine, 1-methylguanosine, N2-methylguanosine, 7-methylguanosine, 2-methylthio-N6-isopentenyl-adenosine and 2-methylthio-N6-threonylcarbamoyl-adenosine (15,16). Particularly, m⁵C widely exists in tRNA, mRNA and long non-coding (lnc)RNA, and mainly impacts the progression of diseases by regulating the export, stability and translation efficiency of mRNA (17-20). Like other RNA methylation types, m⁵C is dynamic and catalyzed by a methyltransferase (writer), removed by demethylase (eraser) and recognized by m⁵C-binding proteins (reader). NOP2/Sun RNA methyltransferase family members 2 and 6 (NSUN2 and NSUN6, respectively) were suggested to be the most important methyltransferases (writer) to catalyze m⁵C (21,22). Previous studies reported that NSUN2 and NSUN6 could regulate the expression of mRNA, tRNA and lncRNA in an m⁵C-dependent manner,

thus affecting the progression of nervous system diseases and different cancers, including hepatocellular carcinoma, bladder cancer, gallbladder carcinoma, and gastric cancer (23-32).

M6A, catalyzed by methyltransferase like 3 (METTL3) and Wilms tumor 1 associated protein (WTAP), were shown to contribute to the progression of OS (2,33). Additionally, METTL3 could promote the progression of OS by improving the stability of differentiation antagonizing non-protein coding RNA (34) and histone deacetylase 5 mRNAs (35), while WTAP could trigger OS tumorigenesis by downregulating HMBOX1 expression (3). Nonetheless, the role of m^5C in the pathogenesis of OS remains unclear. A recent study performed by the current authors demonstrated the impact of epigenetics on OS progression (36). The current study, through bioinformatics analysis, *in vitro* and *in vivo* experiments, found that NSUN6 mainly regulates OS progression by regulating the stability of eukaryotic elongation factor 1 α-2 (EEF1A2) mRNA in an m^5C-dependent manner, which is known to induce OS progression by activating Akt/mTOR signaling pathway (37).

Materials and methods

Bioinformatics analysis. The present study analyzed the datasets for GSE126209 downloaded from the Gene Expression Omnibus (GEO) database (https://www.ncbi.nlm.nih. gov/geo/query/acc.cgi?acc=GSE126209), as well as the transcriptome data and the corresponding survival information contained in TARGET-OS from UCSC-XENA (http://xena. ucsc.edu/). Gencode platform (https://www.gencodegenes. org/) was used and transcripts per kilobase million (TPM) normalization was performed in TARGET-OS. The data were analyzed by the software R 3.6.2 (https://www.r-project.org/).

Cell culture and cell transfection. In this study, human OS cell lines 143b, MG63, HOS, U2-OS, SAOS2 and bone mesenchymal stem cells (BMSCs) were cultured at 37°C in a 5% CO_2 incubator (Thermo Fisher Scientific, Inc.). All cell lines were obtained from the China Centre for Type Culture Collection. The 143b cells were cultured in RPMI-1640 (Gibco; Thermo Fisher Scientific, Inc.; cat. no. 11875119), the MG63 cells were cultured in DMEM (Gibco; Thermo Fisher Scientific, Inc.; cat. no. 12430047), the U2-OS and SAOS2 cells were cultured in McCoy's 5A (Gibco; Thermo Fisher Scientific, Inc.; cat. no. 12330031), the HOS cells were cultured in MEM (Gibco; Thermo Fisher Scientific, Inc.; cat. no. 51200038), the BMSCs were cultured in αMEM (Gibco; Thermo Fisher Scientific, Inc.; cat. no. 41061029), containing 1% penicillin/streptomycin and 10% Fetal Bovine Serum (FBS, Gibco; Thermo Fisher Scientific, Inc.; cat. no. 12484028).

In the section of functional rescue assays, Akt signaling pathway activator SC79 (5 μM; cat. no. SF2730; Beyotime Institute of Biotechnology) was used.

Lentiviruses with puromycin tags were purchased from Hanbio Biotechnology Co., Ltd. The name of the lentiviral plasmid containing shRNA was pHBLV-U6-MCS-EF1-Zs-Green-T2A-Luc. The multiplicity of infection (MOI) used to infect 143b cells was 50, and to infect U2OS cells, the MOI was 30. The cells were stably transfected with NSUN6-knockdown lentiviruses (short-hairpin(sh)-NSUN6#1 and sh-NSUN6#2) and the corresponding negative control (sh-ctrl), as well as with

the EEF1A2-overexpression (OE) lentivirus (OE-EEF1A2) and empty vector negative control (OE-ctrl). The duration of transduction into cells was 24 h, and time interval between transduction and subsequent experimentation was 72 h. Subsequently, puromycin (5 μg/ml) was added to cells to select stably transfected OS cells for further experiments. The following sequences were used for NSUN6-knockdown transfections: sh-NSUN6#1, GAACAAAGGCGGTTAAAC T; sh-NSUN6#2: GCTGCAGCGATTTGATCCA. The sh-ctrl sequence was: 5'-TTCTCCGAACGTGTCACGTdTdT-3'.

Reverse transcription-quantitative PCR (RT-qPCR). Total RNA was extracted from $1x10^6$ cells using TRIzol™ reagent (Invitrogen; Thermo Fisher Scientific, Inc.), according to the manufacturer's instructions. Total RNA was reverse-transcribed into cDNA using a reverse transcriptase kit (HiScript II Q RT SuperMix for qPCR, +gDNA wiper; cat. no. R223; Vazyme Biotech Co., Ltd.) according to the manufacturer's instructions. qPCR was subsequently performed using the ChamQ Universal SYBR qPCR Master Mix (Vazyme Biotech Co., Ltd.), according to the manufacturer's instructions. The thermocycling conditions used for qPCR were as follows: Stage 1, 95°C for 30 sec; stage 2, 95°C for 10 sec and 60°C for 30 sec, for 40 cycles; and stage 3, 95°C for 15 sec, 60°C for 60 sec and 95°C for 15 sec. The mRNA levels were normalized to the reference gene GAPDH. The $2^{-\Delta\Delta Cq}$ equation was applied to calculate the relative expression level (38). The primer pair sequences used for qPCR are listed in Table I.

Cell Counting Kit-8 (CCK-8) and colony formation assay. CCK-8 and colony formation assays were performed to measure the proliferation of stably transfected OS cells. For the CCK-8 assay, cells were seeded in 96-well plates at a density of 2,000 cells/well and the optical density value of each well was detected at 450 nm using a microplate reader at 24, 48 and 72 h after plating. The CCK-8 working fluid was purchased from Beyotime Institute of Biotechnology.

For colony formation assay, OS cells were seeded in 6-well plates at a density of 1,000 cells/well and cultured for 2 weeks. Then, the cells were fixed in 4% paraformaldehyde (Beijing Solarbio Science & Technology Co., Ltd.) at 25°C for 15 min and stained with 1% crystal violet (Beijing Solarbio Science & Technology Co., Ltd.) at 25°C for 15 min. Subsequently, the colonies were photographed and counted. Colonies were defined as >50 cells. The colonies were quantified using ImageJ V2.6 (National Institutes of Health).

Transwell and migration assays. Transwell assays were used to assess cell invasion of stably transfected OS cells, while wound-healing assays were used to evaluate their cell migration. For the Transwell assay, the upper chambers were precoated with Matrigel (Corning, Inc.; pore size 8.0 μm) at room temperature until dry. Cells were seeded in the upper chamber at a density of $2x10^4$ cells/well with culture medium supplemented with 1% FBS, while the bottom chambers contained culture medium supplemented with 20% FBS. After 24 h of incubation at 37°C, the cells in the upper chamber were removed with a cotton swab, while cells invading the lower surfaces of the chambers were fixed in 4% paraformaldehyde (Beijing Solarbio Science & Technology Co., Ltd.) at 25°C

Table I. Primer pair sequences used for reverse transcription-quantitative PCR.

Genes	Forward	Reverse
NOP2/Sun RNA methyltransferase family member 6	5'-TCTCAGCCCTTCATTTGACAGT-3'	5'-TCCAGTGCTATAACTTCTCCCTG-3'
Eukaryotic elongation factor 1 α-2	5'-GAAGACCCACATCAACATCGT-3'	5'-CTCCGCATTTGTAGATGAGGTG-3'
GAPDH	5'-CAAATTCCATGGCACCGTCA-3'	5'-GACTCCACGACGTACTCAGC-3'

for 15 min, and then stained with 1% crystal violet (Beijing Solarbio Science & Technology Co., Ltd.) at 25˚C for 15 min. Stained cells were counted in three randomly selected fields using an optical microscope (ThermoFisher).

For the wound-healing assay, stably transfected $1x10^5$ OS cells were seeded in 6-well plates and an artificial wound was created using a 1,000-μl pipette tip when the cell confluence reached 90%. The cells were then cultured with culture medium containing 1% FBS at 37˚C for 24 h. Images were taken to record the width of the wound at 0 and 24 h. Cell migration was evaluated using the following formula: $(Width_{0h}-width_{24h})/width_{0h}$.

RNA immunoprecipitation (RIP). After mixing with 5 μg of antibody against NSUN6 (Invitrogen; Thermo Fisher Scientific, Inc.; cat. no. PA5-96608) or IgG (Proteintech Group, Inc.; cat. no. 30000-0-AP), magnetic beads (MedChemExpress) were added to OS cell lysates and the mixtures were incubated at 4˚C for 12 h. The lysis buffer was purchased from Thermo Fisher Scientific, Inc. Subsequently, proteinase K digestion buffer was added to digest the complexes for 45 min at 55˚C. After that, extraction buffer (phenol:chloroform:isoamyl alcohol=125:24:1) was used to isolate RNA from the mixture. The extracted RNA was subsequently analyzed using RT-qPCR. IgG was used as a negative control to preclude nonspecific binding.

Methylated-RIP. The protocol used for methylated RIP assay was very similar to that used for RIP. Briefly, ~150 μg of total RNA isolated from stably transfected OS cells was immunoprecipitated with magnetic beads (MedChemExpress) precoated with 10 μg of anti-m^5C antibody (Abcam; cat. no. ab214727). Subsequently, the complexes were digested using proteinase K digestion buffer so that the RNA combined with the antibody could be eluted from the complex. Similarly, buffer (phenol:chloroform:isoamyl alcohol=125:24:1) was used to extract the RNA from the mixture. Then, the extracted RNA was further analyzed using RT-qPCR. The relative m^5C enrichment of mRNA was normalized to the Input, a positive control, which was RNA solution without antibodies added.

Dot blot assay. mRNA was isolated from the total RNA using an mRNA Purification Kit (Beyotime Institute of Biotechnology) and denatured at 65˚C for 5 min. Subsequently, mRNAs were loaded onto an Amersham™ Hybond™ N+ membrane (GE Healthcare). After being crosslinked with ultraviolet light for 5 min, the membrane was stained with 0.02% methylene blue at 25˚C for 5 min (Sangon Biotech Co. Ltd.). Subsequently, the membrane was blocked with 5% non-fat dried milk in PBS with 0.02% Tween-20 (at 25˚C for 1 h) and then incubated with an anti-m^5C antibody (1:1,000, cat. no. ab214727; Abcam) overnight at 4˚C. Following primary incubation, the membrane was incubated with the secondary antibody (1:5,000; cat. no. PR30011; Proteintech Group, Inc.), the membrane was visualized with an Odyssey Infrared Imaging System (LI-COR Biosciences).

mRNA stability assay. To analyze mRNA stability, stably transfected OS cells were treated with actinomycin D (ActD, 5 μg/ml). Subsequently, the cells were collected by scraping them from the plates and total RNA was extracted using TRIzol reagent at different time points (0, 1, 2 and 4 h after ActD treatment). Thereafter, mRNA content was measured using RT-qPCR. The mRNA remaining was normalized to the expression at 0 h.

Western blotting. Total proteins were extracted from OS cells with IP cell lysate (Thermo Fisher Scientific, Inc.), quantified by BCA assay (Beyotime Institute of Biotechnology) and then separated by SDS-PAGE on a 10% gel. The separated proteins were subsequently transferred onto PVDF membranes (Beyotime Institute of Biotechnology). Next, the membranes were blocked with 5% fat-free milk powder (Beyotime Institute of Biotechnology) at 25˚C for 2 h. The membranes were incubated with primary antibodies at 4˚C for 12 h, followed by incubation with secondary antibodies (goat anti-rabbit; 1:5,000; cat. no. PR30011; Proteintech Group, Inc.) for 1 h at room temperature after washes. Subsequently, protein band visualization was performed using an Odyssey Infrared Imaging System (LI-COR Biosciences) and quantified using ImageJ software V2.6 (National Institutes of Health). Detailed information about the primary antibodies is provided in Table II.

Tumor xenograft model. The animal study was approved by the Ethics Committee of Zhongnan Hospital of Wuhan University (approval no. WQ20210015). A total of 18 4-week-old male BALB/c nude mice were purchased from GemPharmatech Co., Ltd. All the mice were evenly divided into three groups: Sh-ctrl; sh-NSUN6#1; and sh-NSUN6#2. Stably transfected 143b cells were collected and then resuspended in PBS (approximately 10^7/ml). Next, 100 μl of cells (containing ~10^6 cells) was injected into the upper right side of each mouse's back. Then the health status of each mouse and measured the size of each tumor were monitored every two days. Mice with tumor tissue diameter >20 mm were euthanized. Mice were observed for a total of 3 weeks and no mice were euthanized in advance. After 3 weeks, all 18 mice

Table II. Detailed information about primary antibodies.

Antibodies	Manufacturer (cat. no.)	Dilution
NOP2/Sun RNA methyltransferase family member 6	Proteintech Group, Inc. (17240-1-AP)	1:1,000
Eukaryotic elongation factor 1 α-2	Proteintech Group, Inc. (16091-1-AP)	1:1,000
P-AKT	Proteintech Group, Inc. (66444-1-Ig)	1:1,000
AKT	Proteintech Group, Inc. (60203-2-Ig)	1:1,000
P-mTOR	Proteintech Group, Inc. (67778-1-Ig)	1:1,000
mTOR	Proteintech Group, Inc. (66888-1-Ig)	1:1,000
c-Myc	Proteintech Group, Inc. (10828-1-AP)	1:1,000
P21	Proteintech Group, Inc. (10355-1-AP)	1:1,000
GAPDH	Proteintech Group, Inc. (60004-1-Ig)	1:1,000
5-methylcytidine methyltransferase	Abcam (ab214727)	1:1,000

P, phosphorylated.

were euthanized and all the tumor tissues were harvested. To minimize the suffering and distress of the mice, the mice were euthanized with an intraperitoneal injection of pentobarbital sodium at a dose of 150 mg/kg. Death was confirmed when the mouse lost breathing and lost its response after being stimulated. Subsequently, all the tumor tissues were weighed and measured, and the volume of each tumor was calculated using the formula: Tumor volume (mm^3)=length x width^2 x 0.5. Immunohistochemical analysis of the tumor tissues was performed by Wuhan Servicebio Technology Co., Ltd.

Statistical analysis. In this study, all data are presented as mean ± standard deviation from three independent experiments. Statistical significance was determined using one-way ANOVA or unpaired two-tailed Student's t-test. To compare >2 groups one-way ANOVA was used followed by Bonferroni multiple comparisons post hoc test. Statistical analysis was performed with GraphPad Prism 8.0 (GraphPad Software; Dotmatics). P<0.05 was considered to indicate a statistically significant difference.

Results

NSUN6 is highly expressed in osteosarcoma. To characterize the expression profile of NSUN6 in human OS, the data of GSE126209 from the GEO database were first analyzed and the results showed that NSUN6 expression was higher in osteosarcomas tumors than that in the adjacent normal tissues (Fig. 1A). Subsequently, RT-qPCR and Western Blot assays were performed to validate NSUN6 expression in OS cell lines and bone mesenchymal stem cells (BMSCs). Results from both assays showed that the NSUN6 expression was increased in OS cell lines compared with that in BMSCs (Fig. 1B and C). In addition, after analyzing the transcriptome data and corresponding survival information in TARGET-OS from UCSC-XENA (http://xena.ucsc.edu/), it was observed that higher NSUN6 expression was correlated with poorer prognosis in patients with OS (Fig. 1D). Collectively, these results indicate that NSUN6 is highly expressed in human OS and may contribute to poor prognosis.

NSUN6 deficiency significantly inhibits OS progression in vitro. To explore the functional roles of NSUN6 in OS progression, stable NSUN6-knockdown OS cell lines were generated by transfecting 143b and U2-OS cells with lentivirus encoding sh-NSUN6#1 and sh-NSUN6#2; thereafter proliferation, invasion and migration of these cells were examined. NSUN6 expression was successfully downregulated in these cells when compared with the control group (sh-ctrl) (Fig. 2A). As shown through the CCK-8 and colony formation assays, the knockdown of NSUN6 inhibited the proliferation of OS cells (Fig. 2B and C). Interestingly, overexpressing NSUN6 in BMSC (Fig. S1A) could enhance proliferation and colony formation, mimicking the cancerous phenotype of OS cells (Fig. S1B and C). Furthermore, knocking down NSUN6 significantly attenuated the invasion and migration of OS cells, as evidenced by results from Transwell and wound-healing assays, respectively (Fig. 2D and E). Overall, the aforementioned findings indicated that NSUN6 deficiency could suppress OS progression *in vitro*.

EEF1A2 is the potential target of NSUN6 in human OS. To dissect the underlying molecular mechanism of NSUN6-mediated OS progression, the data in TARGET-OS from UCSC-XENA (http://xena.ucsc.edu/) were analyzed to screen for downstream targets of NSUN6. First, all the patients in TARGET-OS were divided into the 'high NSUN6' group and 'low NSUN6' group using the median value of NSUN6 expression. Subsequently, all genes were screened using two criteria: P<0.05; and the absolute value of Log$_2$(Fold Change) >1. The following four target genes with the largest fold changes were identified: EEF1A2; melanoma antigen preferentially expressed in tumors (PRAME); fibroblast growth factor binding protein 2 (FGFBP2); and TP53 (Fig. 3A). Further analysis revealed that EEF1A2 expression had the strongest correlation with the expression of NSUN6 (P=0.0017) (Fig. 3B-E). This finding was further validated experimentally; the expression of EEF1A2 mRNA was substantially reduced in cells transfected with sh-NSUN6#1 and sh-NSUN6#2 lentivirus (Fig. 3F and G). Lastly, a RIP assay was performed to determine whether NSUN6 regulated EEF1A2 expression through direct or
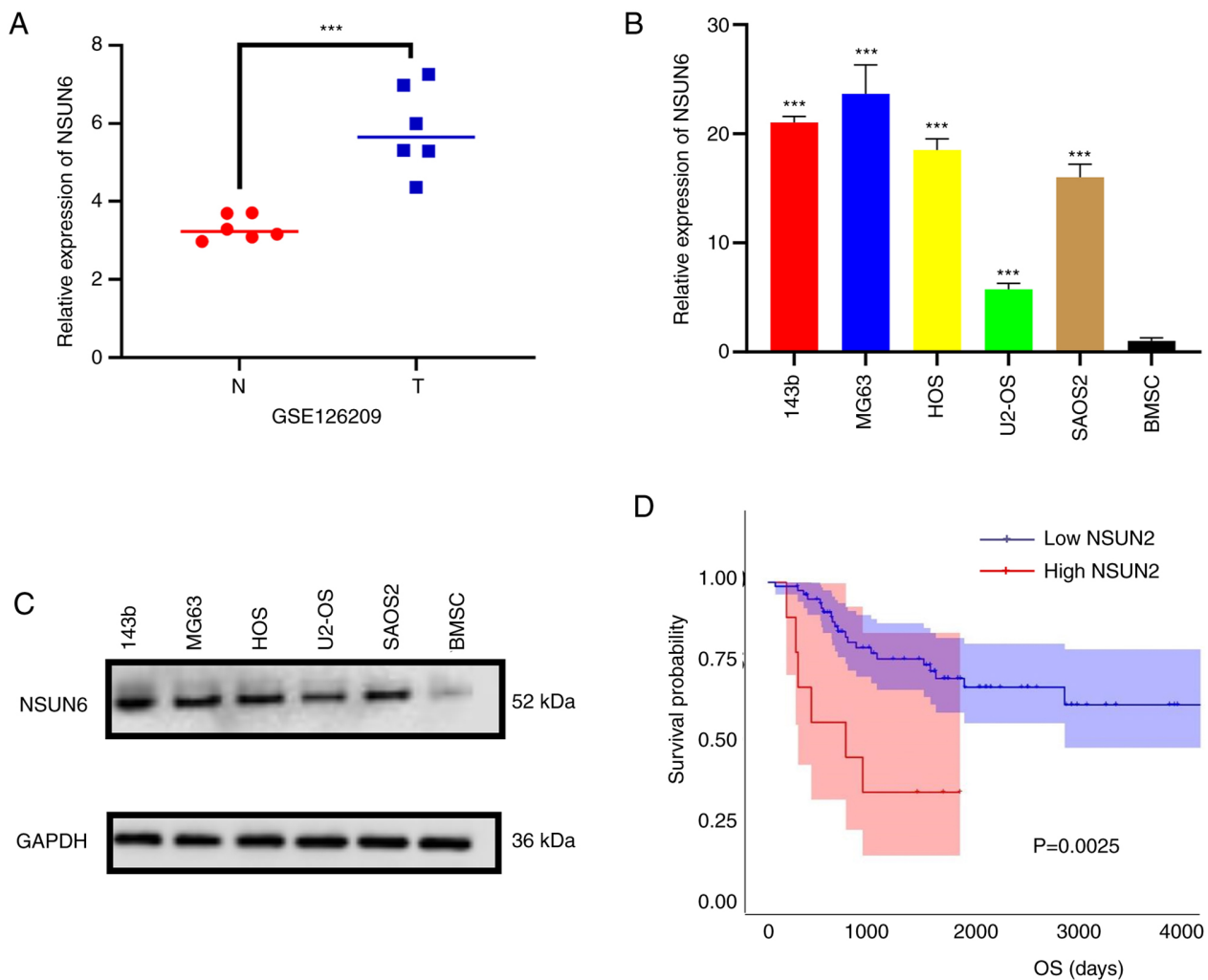
Figure 1. NSUN6 is highly expressed in OS. (A) Data from the Gene Expression Omnibus database (accession no. GSE126209) confirmed that the expression of NSUN6 in OS tissues was higher than that in the adjacent normal tissues. (B) Reverse transcription-quantitative PCR and (C) Western blotting results indicate the mRNA and protein expression levels of NSUN6 in OS cell lines and BMSCs, respectively. (D) Survival analysis of NSUN6 expression in patients with OS from UCSC-XENA database. Patients were divided into high- and low-NSUN6 expressions using the software R 3.6.2. ***P<0.001. NSUN6, NOP2/Sun RNA methyltransferase family member 6; OS, osteosarcoma.

indirect action. The result of the RIP assay showed that EEF1A2 mRNA could be pulled down with NUSN6 antibody, indicating that NSUN6 protein could directly bind to EEF1A2 mRNA (Fig. 3H and I). Collectively, these data suggested that EEF1A2 expression is positively correlated with the expression of NSUN6, which could directly bind to EEF1A2 mRNA.

NSUN6 regulates the stability of EEF1A2 mRNA via m⁵C. Given that NSUN6 is a well-known methylase with a function to induce m^5C modification (22), a Dot Plot assay was performed to evaluate whether NSUN6 could regulate the m^5C level in OS cells. As shown in Fig. 4A and B, the knockdown of NSUN6 led to a decreased level of m^5C in 143b and U2-OS cells. Since EEF1A2 mRNA was confirmed as a direct target of NSUN6, a methylated-RIP assay was utilized to further explore whether NSUN6 could regulate EEF1A2 expression by modulating the m^5C level of EEF1A2 mRNA. The results confirmed the presence of m^5C modification on EEF1A2 mRNA; more importantly, loss of NSUN6 resulted in less m^5C modification of EEF1A2 mRNA (Fig. 4C and D).

A previous study demonstrated that NSUN6 primarily targets the consensus sequence motif CTCCA on the 3'-untranslated region of mRNA, which is mainly related to mRNA stability (39); therefore, the present study evaluated whether NSUN6 affects EEF1A2 mRNA stability. The current data showed a faster degradation rate of EEF1A2 mRNA in sh-NSUN6#1 and sh-NSUN6#2 groups, when compared with the sh-ctrl group (Fig. 4E and F), suggesting that loss of NSUN6 reduced the stability of EEF1A2 mRNA in 143b and U2-OS cells. Altogether, the aforementioned results revealed that NSUN6 could bind to EEF1A2 mRNA and regulate its m^5C modification, thus regulating the stability of EEF1A2 mRNA in OS.

Loss of NSUN6 reduced the activation of the Akt/mTOR signaling pathway in OS. A previous report showed that EEF1A2 could promote the progression of OS by activating Akt/mTOR signaling pathway (37). Thus, the present study aimed to evaluate whether the Akt/mTOR signaling pathway is a downstream effector of the NSUN6/EEF1A2 signaling in OS. The level of NSUN6 protein was significantly decreased
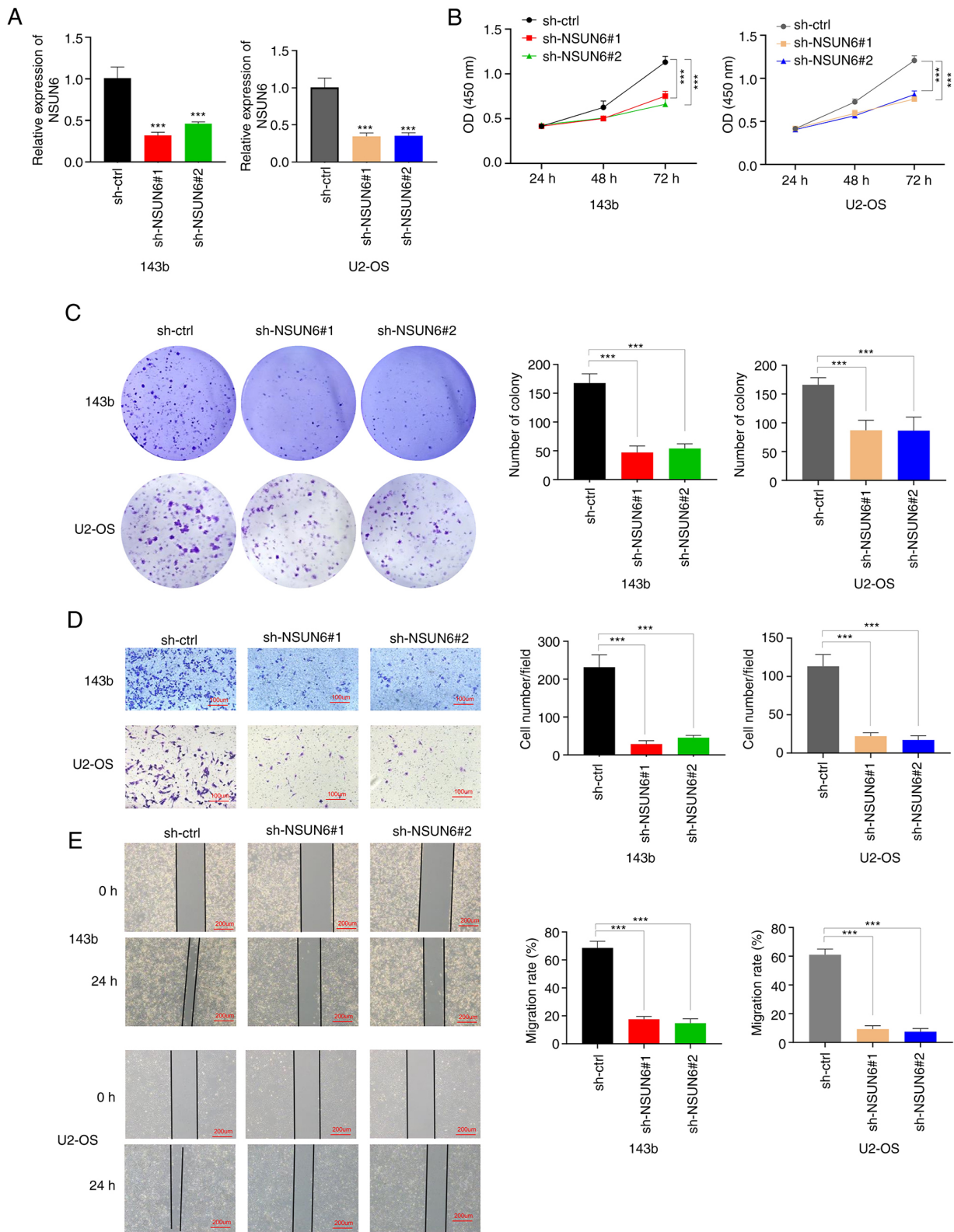
Figure 2. NSUN6 deficiency significantly inhibits OS progression *in vitro*. (A) The expression of NSUN6 mRNA in sh-ctrl, sh-NSUN6#1 and sh-NSUN6#2 groups of 143b and U2-OS cells. Results of (B) Cell Counting Kit-8, (C) Colony formation, (D) Transwell (scale bar, 100 μM) and (E) Wound-healing (scale bar, 200 μM) assays. ***P<0.001. NSUN6, NOP2/Sun RNA methyltransferase family member 6; OS, osteosarcoma; sh, short-hairpin; ctrl, control; OD, optical density.

following sh-NSUN6#1 and sh-NSUN6#2 transfections in 143b and U2-OS cells (Fig. 5A and B). This was accompanied by a significant decrease in protein levels of EEF1A2 and c-Myc, and phosphorylation of Akt and mTOR; whereas p21 protein levels were increased in NSUN6-deficient OS cells (Fig. 5A and B). Taken together, NSUN6 knockdown decreased the expression of EEF1A2 protein and consequently suppressed Akt/mTOR signaling pathway.
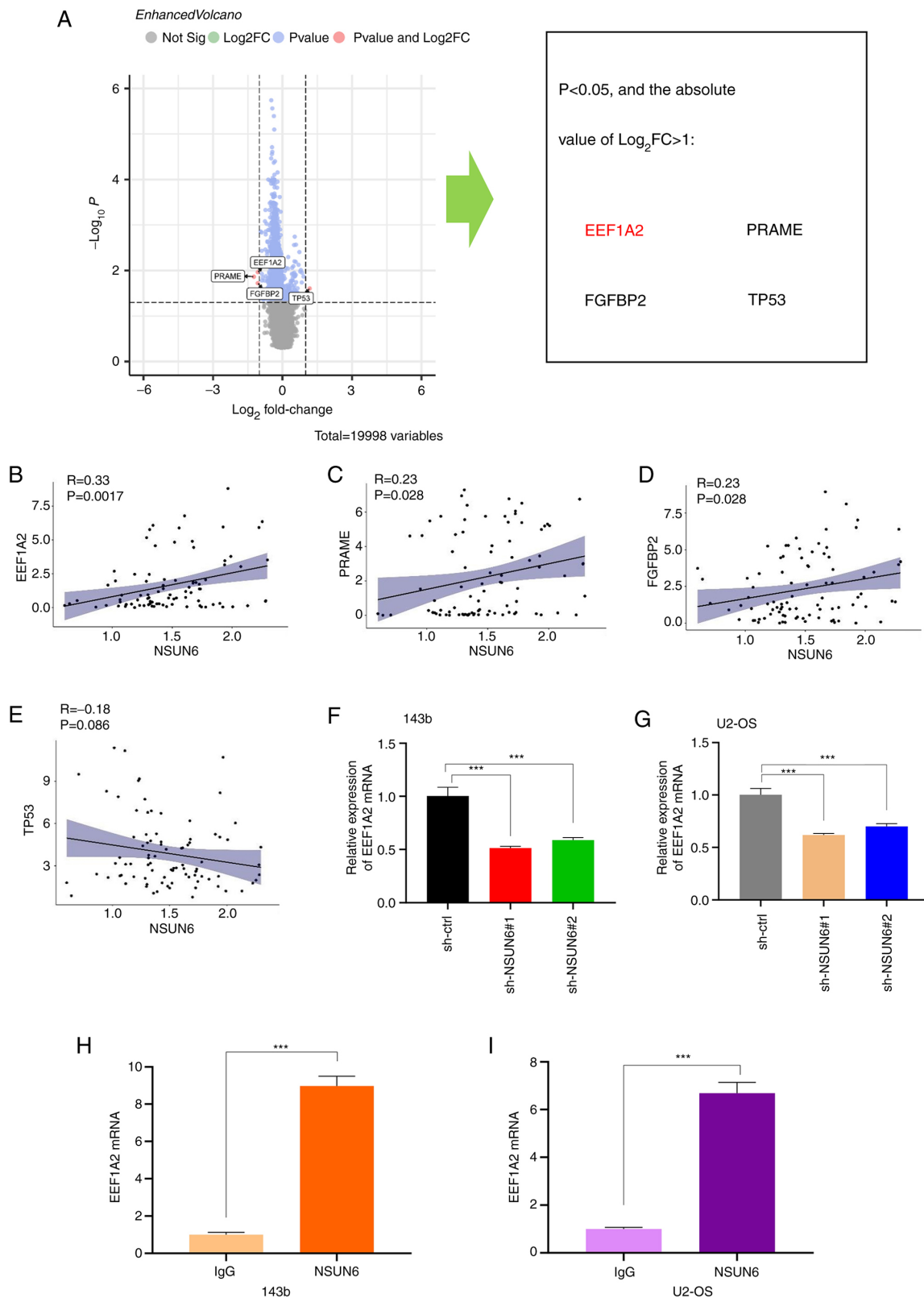
Figure 3. EEF1A2 is the potential target of NSUN6 in human OS. (A) Volcano plot showing that expression difference of EEF1A2, PRAME, FGFBP2 and TP53 was the largest between high- and low-NSUN6 groups. Correlation of NSUN6 with (B) EEF1A2 (P=0.0017), (C) PRAME (P=0.028), (D) FGFBP2 (P=0.028) and (E) TP53 (P=0.086) in human OS. Expression of EEF1A2 mRNA in sh-ctrl, sh-NSUN6#1 group and sh-NSUN6#2 groups of (F) 143b and (G) U2-OS cells. RIP assay results in (H) 143b and (I) U2-OS cells. IgG was used as a negative control. ***P<0.001. NSUN6, NOP2/Sun RNA methyltransferase family member 6; OS, osteosarcoma; EEF1A2, eukaryotic elongation factor 1 α-2; PRAME, melanoma antigen preferentially expressed in tumors; FGFBP2, fibroblast growth factor binding protein 2; sh, short-hairpin; ctrl, control.

Loss of NSUN6 inhibits the proliferation of OS in vivo. To evaluate whether NSUN6 could regulate the proliferation of OS *in vivo*, tumor xenografts in 4-week-old nude mice were generated using stably transfected 143b cells. The mice were
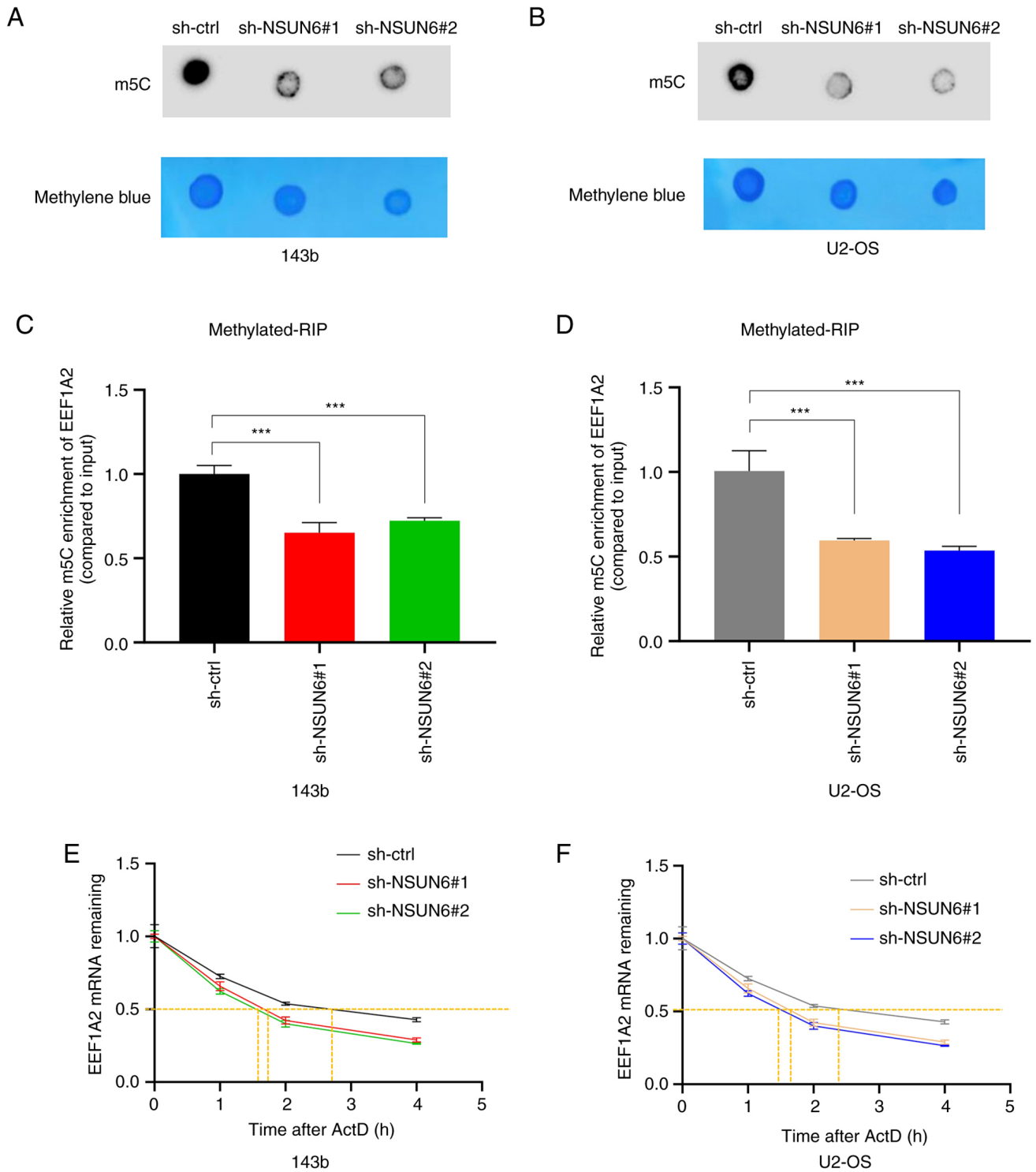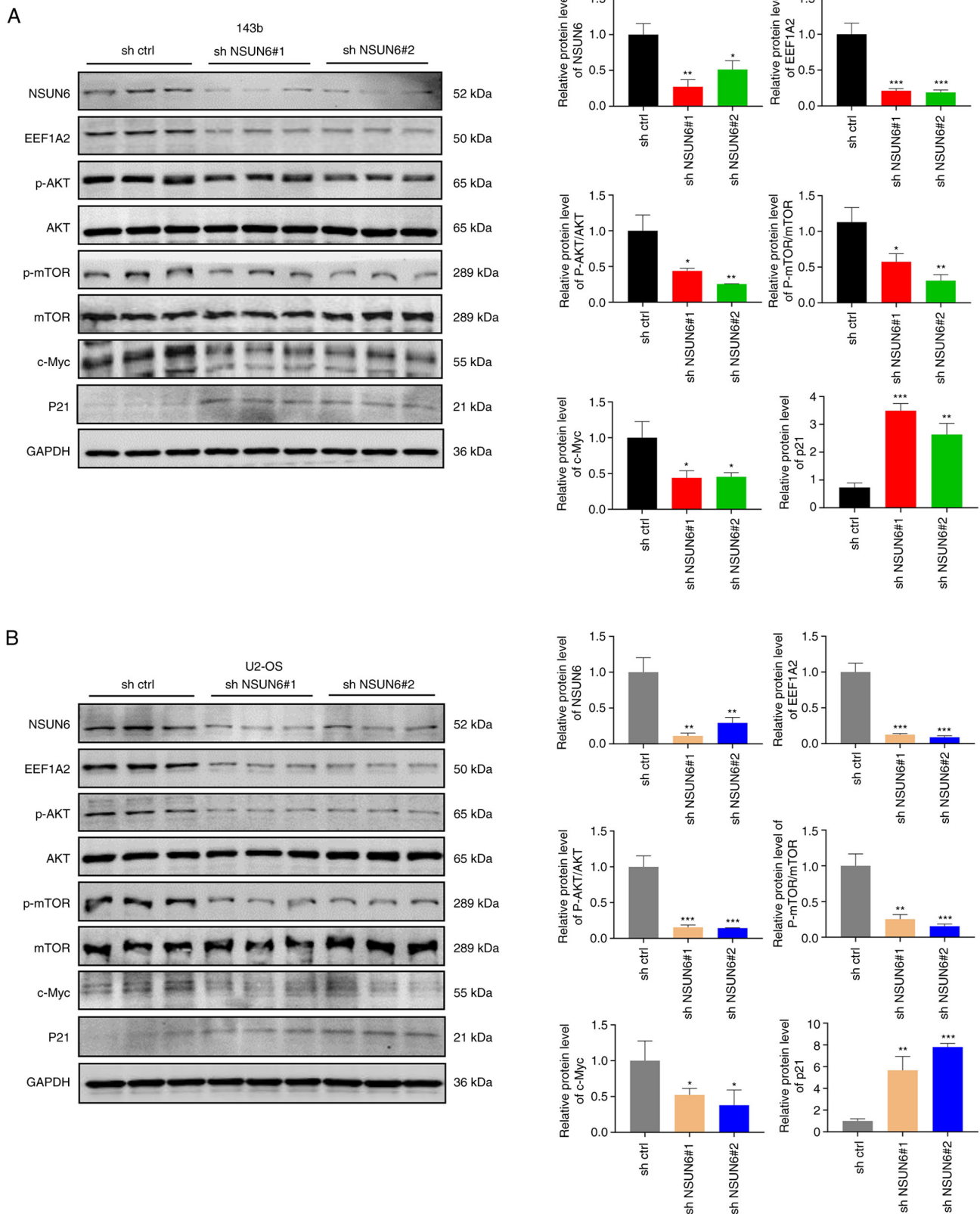
Figure 4. NSUN6 regulates the stability of EEF1A2 mRNA via m⁵C modification. Dot Blot assay of (A) 143b and (B) U2-OS cells. Methylene blue staining (lower image) was used to detect the amount of RNA loaded, while the intensity of dot immunoblotting (upper image) represented the level of m⁵C modification. Methylated-RIP was used to detect the m⁵C modification level of EEF1A2 mRNA of (C) 143b and (D) U2-OS cells. Curves of EEF1A2 mRNA remaining vs. time after ActD treatment in (E) 143b and (F) U2-OS cells. ***P<0.001. NSUN6, NOP2/Sun RNA methyltransferase family member 6; OS, osteosarcoma; EEF1A2, eukaryotic elongation factor 1 α-2; RIP, RNA immunoprecipitation; m⁵C, 5-methylcytidine; sh, short-hairpin; ctrl, control.

euthanized 3 weeks after the 143b cells were inoculated and tumor tissue was harvested from each mouse for further examination. As shown in Fig. 6A-D, the tumor size, weight and volume were smaller in mice in the sh-NSUN6#1 and sh-NSUN6#2 groups compared with those in the sh-ctrl group. In addition, the immunostaining results showed that protein levels of NSUN6, EEF1A2 and Ki-67 were all significantly lower in the tumors from mice injected with NSUN6-knockdown OS cells compared with those in the control group (Fig. 6E). Overall, the aforementioned results suggested a blunted tumor progression *in vivo* when NSUN6 was knocked down.

Figure 5. Loss of NOP2/Sun RNA methyltransferase family members 6 reduced the activation of the Akt/mTOR signaling pathway in OS. (A) The results of western blot assay and statistical chart for 143b cell. (B) The results of western blot assay and statistical chart for U2-OS cell. *P<0.05, **P<0.01 and ***P<0.001. P, phsophorylated; NSUN6, NOP2/Sun RNA methyltransferase family member 6; EEF1A2, eukaryotic elongation factor 1 α-2; sh, short-hairpin; ctrl, control.

EEF1A2 overexpression or Akt signaling pathway activator SC79 can counterbalance the inhibitory effects of NSUN6 deficiency on OS progression. To further validate the functional roles of EEF1A2 and Akt/mTOR signaling pathway action on OS suppression triggered by NSUN6 deficiency, functional rescue assays were performed in 143b cells by overexpressing EEF1A2 or stimulating cells with Akt signaling pathway activator SC79. As is shown
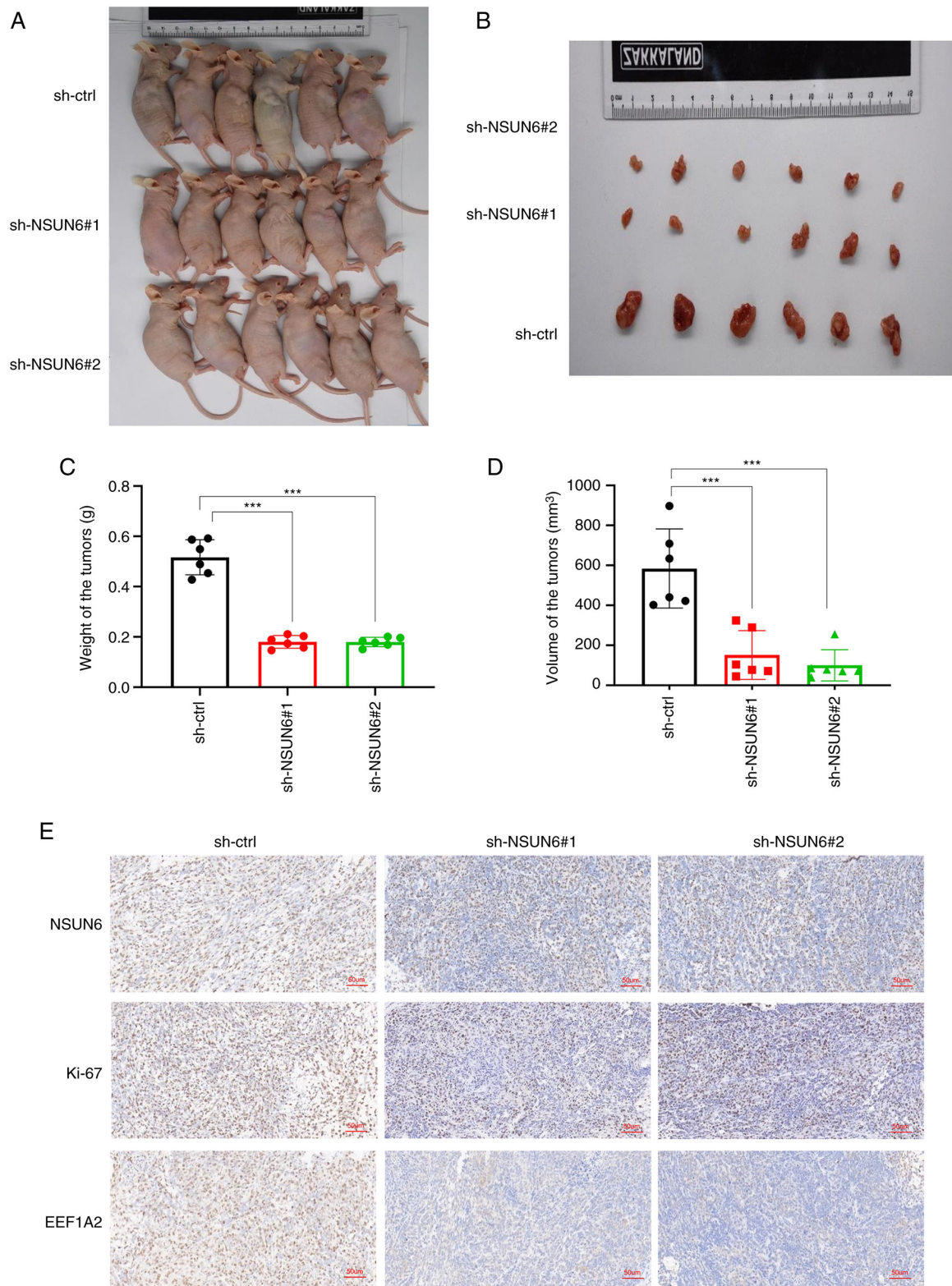
Figure 6. Loss of NOP2/Sun RNA methyltransferase family members 6 inhibits the proliferation of osteosarcoma *in vivo*. (A) Representative image of all the nude mice from different groups. The tumors were on the nude mice. (B) Representative images of all the tumors collected from nude mice from different groups. (C) Weight and (D) Volume of all the tumors. (E) Result of immunohistochemistry (scale bar, 50 μM). ***P<0.001. EEF1A2, eukaryotic elongation factor 1 α-2; sh, short-hairpin; ctrl, control.

in Fig. S2, lentiviral transfection successfully increased EEF1A2 mRNA expression in 143b cells, while an empty vector was used as OE-ctrl. Meanwhile, SC79 treatment showed no effect on EEF1A2 gene expression (Fig. 7A). In Fig. 7, the cells transfected with sh-ctrl lentiviral were used as control. Importantly, both EEF1A2 overexpression and SC79 stimulation improved the proliferation of 143b cells, as shown using CCK-8 and colony formation assays (Fig. 7B and C).
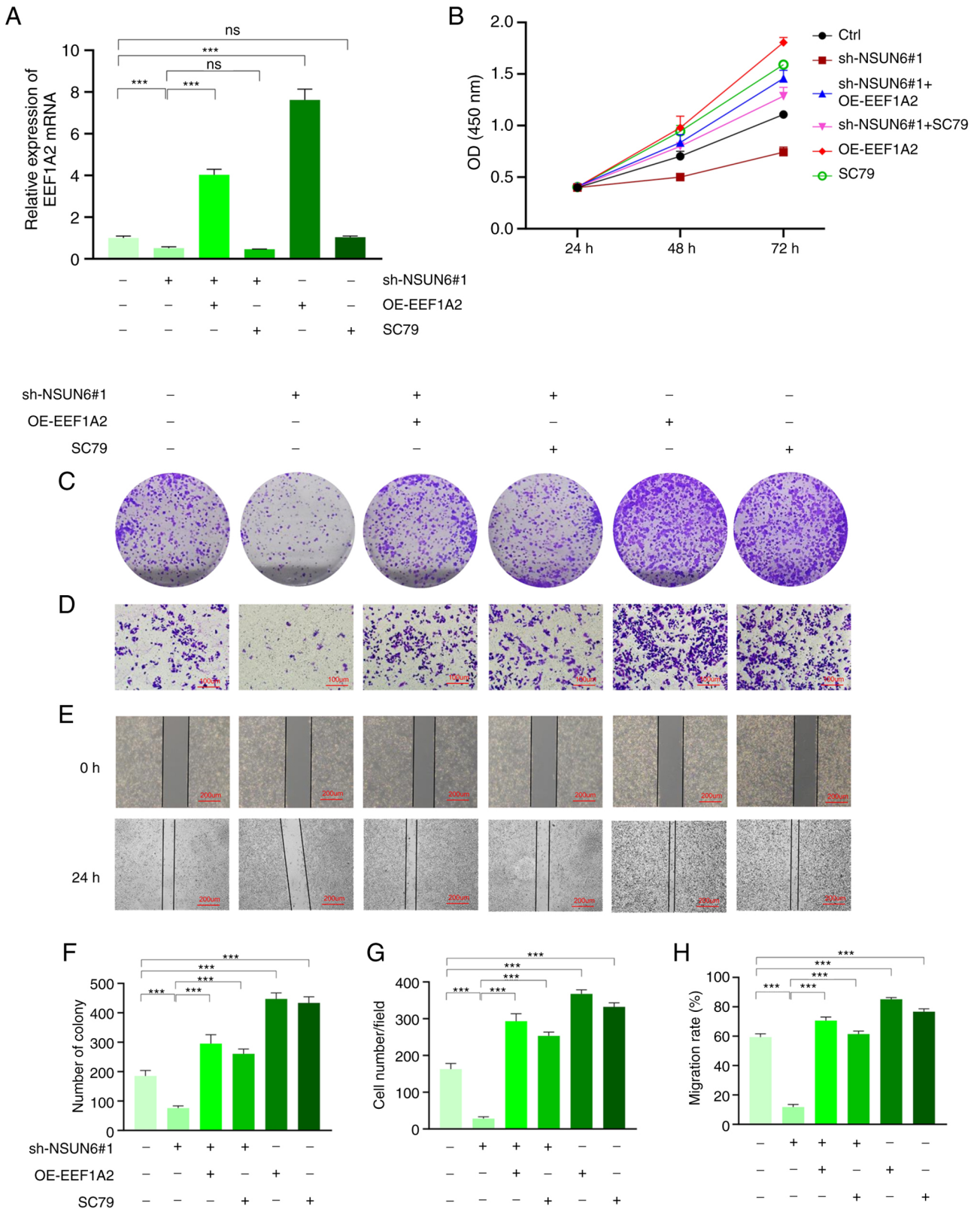
Figure 7. EEF1A2 overexpression and Akt signaling pathway activator SC79 can counterbalance the inhibition of NSUN6 deficiency on OS progression. (A) Results of reverse transcription-quantitative PCR showing the expression level of EEF1A2 mRNA in 143b cells of different groups. Results of (B) Cell Counting Kit-8, (C) Colony formation, (D) Transwell (scale bar, 100 μM) and (E) Wound-healing assays (scale bar, 200 μM). Statistical charts of (F) Colony formation, (G) Transwell, and (H) Wound-healing assay. ***P<0.001. NSUN6, NOP2/Sun RNA methyltransferase family member 6; EEF1A2, eukaryotic elongation factor 1 α-2; sh, short-hairpin; OE, overexpression; ctrl, control.

In addition, the results of the Transwell and wound-healing assays demonstrated that EEF1A2 overexpression and SC79 administration significantly increased 143b cell invasion and migration (Fig. 7D and E). Statistical chart of colony

formation, Transwell and wound-healing assays are shown in Fig. 7 F-H. Collectively, the present results indicated that EEF1A2 overexpression or Akt/mTOR signaling pathway action could blunt the beneficial effect of NSUN6 knockdown on suppressing OS progression.

Discussion

Currently, the primary treatment approach for OS involves a combination of chemotherapy and surgery. However, OS has a high propensity to metastasize to the lungs in a relatively short time, leading to a significant number of cases where patients with OS are diagnosed with pre-existing lung metastases, thereby eliminating the possibility of surgical intervention (1,2). This underscores the need for more effective treatment strategies that can prevent or mitigate OS progression to distant sites, particularly the lungs (1). The efficacy of the current therapeutic approaches is limited due to the onset of adverse effects, development of chemotherapy resistance and high rates of relapse (5). To address this challenge, there is a pressing need for in-depth studies that can elucidate the molecular mechanisms involved in OS pathogenesis because these findings may reveal novel therapeutic targets that can be exploited to develop more effective treatments for OS.

Accumulating evidence demonstrated that RNA methylation modification could contribute to the pathogenesis of various diseases, especially in cancer (16,40). Among different RNA modifications, m6A has been extensively studied in cancer progression and molecular mechanism, whereas the roles of m5C have been relatively neglected (41,42). Preliminary studies suggested that m5C modification solely occurred on tRNA (18,19); however, more mature studies showed that m5C modification could also occur on mRNA, significantly impacting mRNA metabolism, including export, stability and translation efficiency (17,18,20,43-45). A previous study reported that m5C modification, induced by NSUN2 and recognized by YBX1, could promote the pathogenesis of bladder cancer by stabilizing different mRNA targets (24). Furthermore, NSUN2 was also shown to promote cancer progression by destabilizing p57Kip2 mRNA or stabilizing growth factor receptor-bound protein 2 mRNA via m5C modification, and enhancing Autotaxin mRNA translation (27,46,47).

As another important methyltransferase that induces m5C modification, NSUN6 was found to suppress pancreatic cancer development by regulating cell proliferation (28). Despite numerous studies (19,21,22) highlighting the critical role of m5C modification induced by NSUN2 or NSUN6 in various cancer types, its function in OS progression remains unclear. A previous study from the present authors indicated a high expression level of NSUN2 in OS cells (36). In addition, the current study found that NSUN6 was highly expressed in OS, which was associated with poorer prognosis in patients with OS. It is plausible that NSUN6 DNA undergoes various chemical modifications during OS progression (i.e. acetylation or lactate), which loosens its binding to histone resulting in higher transcription efficiency. Further research is required to dissect the underlying mechanisms involved in the upregulation of USUN6 expression in OS progression.

The present findings further revealed that the down-regulation of NSUN6 in OS cells could inhibit cancer cell proliferation, invasion and migration. Bioinformatics analysis showed that EEF1A2 has the strongest correlation with NSUN6. Mechanistically, the present study demonstrated that NSUN6 protein could directly bind to EEF1A2 mRNA and the knockdown of NSUN6 led to reduced EEF1A2 mRNA stability via m5C modification. Importantly, EEF1A2 was previously reported to be involved in the pathogenesis of various cancers by enhancing TGF-β/SMAD signaling, binding to protein kinase R and modulating its activity or modulating apoptosis (48-51). Specifically concerning OS progression, Yang *et al* (37) has reported that EEF1A2 promotes OS progression via activating Akt/mTOR pathway. In line with this finding, the present data showed that NSUN6 deficiency decreased the phosphorylation level of Akt/mTOR in OS cells. Furthermore, EEF1A2 overexpression or Akt signaling pathway activation through SC79 stimulation could counterbalance the inhibitory effects of NSUN6 deficiency on OS progression.

Overall, the aforementioned results indicated that NSUN6 could contribute to OS progression by upregulating EEF1A2 and activating Akt/mTOR pathway. Lastly, further research is needed to identify the 'reader' that recognizes the target mRNA methylated by NSUN6.

The current study provided important insights into the molecular mechanisms of OS progression and highlights NSUN6 as a potential therapeutic target for OS. By identifying the role of NSUN6 in regulating the Akt/mTOR signaling pathway, the present findings could potentially inform the development of new treatment strategies for patients with OS.

Availability of data and materials

The datasets used and/or analyzed during the current study are available from the corresponding author on reasonable request.

Authors' contributions

SH and MY performed most of the experiments and wrote the manuscript. KX performed the bioinformatics analysis, designed the cell experiments, and helped SH and MY perform western blot assay and write the manuscript. ZY performed the CCK-8, Transwell and wound-healing assays. LC helped RW design the study and checked the manuscript. YX provided the funding, designed animal experiments, and helped SH and MY perform the animal experiments. LW helped RW design the study, and helped SH and MY write and revise the manuscript. RW designed and supervised the study. SH and MY confirm the authenticity of all the raw data. All authors have read and approved the final manuscript.

Ethics approval and consent to participate

The animal study was approved by the Ethics Committee of Zhongnan Hospital of Wuhan University (approval no. WQ20210015; Wuhan, China).

Patient consent for publication

Not applicable.

Competing interests

The authors declare that they have no competing interests.

References

1. Durfee RA, Mohammed M and Luu HH: Review of osteosarcoma and current management. Rheumatol Ther 3: 221-243, 2016.
2. Li S, Zhang H, Liu J and Shang G. Targeted therapy for osteosarcoma: A review. J Cancer Res Clin Oncol: Feb 18, 2023 (Epub ahead of print).
3. Chen S, Li Y, Zhi S, Ding Z, Wang W, Peng Y, Huang Y, Zheng R, Yu H, Wang J, et al: WTAP promotes osteosarcoma tumorigenesis by repressing HMBOX1 expression in an m6A-dependent manner. Cell Death Dis 11: 659, 2020.
4. Xie L, Yao Z, Zhang Y, Li D, Hu F, Liao Y, Zhou L, Zhou Y, Huang Z, He Z, et al: Deep RNA sequencing reveals the dynamic regulation of miRNA, lncRNAs, and mRNAs in osteosarcoma tumorigenesis and pulmonary metastasis. Cell Death Dis 9: 772, 2018.
5. Jafari F, Javdansirat S, Sanaie S, Naseri A, Shamekh A, Rostamzadeh D and Dolati S: Osteosarcoma: A comprehensive review of management and treatment strategies. Ann Diagn Pathol 49: 151654, 2020.
6. Wang B, Yao L, Dong Y, Liu J and Wu J: LncRNA PCED1B-AS1 knockdown inhibits osteosarcoma via methylation-mediated miR-10a downregulation. J Orthop Surg Res 17: 464, 2022.
7. Tsukamoto S, Righi A, Kido A, Honoki K, Tanaka Y, Fujii H, Mavrogenis AF, Tanaka Y and Errani C: Effect of adjuvant chemotherapy on periosteal osteosarcoma: A systematic review. Jpn J Clin Oncol 52: 896-904, 2022.
8. Liu W, Zhao Y, Wang G, Feng S, Ge X, Ye W, Wang Z, Zhu Y, Cai W, Bai J and Zhou X: TRIM22 inhibits osteosarcoma progression through destabilizing NRF2 and thus activation of ROS/AMPK/mTOR/autophagy signaling. Redox Biol 53: 102344, 2022.
9. Lin H, Chen X, Zhang C, Yang T, Deng Z, Song Y, Huang L, Li F, Li Q, Lin S and Jin D: EF24 induces ferroptosis in osteosarcoma cells through HMOX1. Biomed Pharmacother 136: 111202, 2021.
10. Xiao X, Wang W, Li Y, Yang D, Li X, Shen C, Liu Y, Ke X, Guo S and Guo Z: HSP90AA1-mediated autophagy promotes drug resistance in osteosarcoma. J Exp Clin Cancer Res 37: 201, 2018.
11. Liu Q and Wang K: The induction of ferroptosis by impairing STAT3/Nrf2/GPx4 signaling enhances the sensitivity of osteosarcoma cells to cisplatin. Cell Biol Int 43: 1245-1256, 2019.
12. Dong S, Wu Y, Liu Y, Weng H and Huang H: N6 -methyladenosine steers RNA metabolism and regulation in cancer. Cancer Commun (Lond) 41: 538-559, 2021.
13. Kumar VE, Nambiar R, De Souza C, Nguyen A, Chien J and Lam KS: Targeting epigenetic modifiers of tumor plasticity and cancer stem cell behavior. Cells 11: 1403, 2022.
14. Nacev BA, Jones KB, Intlekofer AM, Yu JSE, Allis CD, Tap WD, Ladanyi M and Nielsen TO: The epigenomics of sarcoma. Nat Rev Cancer 20: 608-623, 2020.
15. Yang B, Wang JQ, Tan Y, Yuan R, Chen ZS and Zou C: RNA methylation and cancer treatment. Pharmacol Res 174: 105937, 2021.
16. Han X, Wang M, Zhao YL, Yang Y and Yang YG: RNA methylations in human cancers. Semin Cancer Biol 75: 97-115, 2021.
17. Dominissini D and Rechavi G: 5-methylcytosine mediates nuclear export of mRNA. Cell Res 27: 717-719, 2017.
18. Garcia-Vilchez R, Sevilla A and Blanco S: Post-transcriptional regulation by cytosine-5 methylation of RNA. Biochim Biophys Acta Gene Regul Mech 1862: 240-252, 2019.
19. Xue C, Zhao Y and Li L: Advances in RNA cytosine-5 methylation: Detection, regulatory mechanisms, biological functions and links to cancer. Biomark Res 8: 43, 2020.
20. Yang X, Yang Y, Sun BF, Chen YS, Xu JW, Lai WY, Li A, Wang X, Bhattarai DP, Xiao W, et al: 5-methylcytosine promotes mRNA export-NSUN2 as the methyltransferase and ALYREF as an m5C reader. Cell Res 27: 606-625, 2017.
21. Chellamuthu A and Gray SG: The RNA methyltransferase NSUN2 and its potential roles in cancer. Cells 9: 1758, 2020.
22. Zhang Q, Liu F, Chen W, Miao H, Liang H, Liao Z, Zhang Z and Zhang B: The role of RNA m5C modification in cancer metastasis. Int J Biol Sci 17: 3369-3380, 2021.
23. Sun Z, Xue S, Zhang M, Xu H, Hu X, Chen S, Liu Y, Guo M and Cui H: Aberrant NSUN2-mediated m5C modification of H19 lncRNA is associated with poor differentiation of hepatocellular carcinoma. Oncogene 39: 6906-6919, 2020.
24. Chen X, Li A, Sun BF, Yang Y, Han YN, Yuan X, Chen RX, Wei WS, Liu Y, Gao CC, et al: 5-methylcytosine promotes pathogenesis of bladder cancer through stabilizing mRNAs. Nat Cell Biol 21: 978-990, 2019.
25. Gao Y, Wang Z, Zhu Y, Zhu Q, Yang Y, Jin Y, Zhang F, Jiang L, Ye Y, Li H, et al: NOP2/Sun RNA methyltransferase 2 promotes tumor progression via its interacting partner RPL6 in gallbladder carcinoma. Cancer Sci 110: 3510-3519, 2019.
26. Hu Y, Chen C, Tong X, Chen S, Hu X, Pan B, Sun X, Chen Z, Shi X, Hu Y, et al: NSUN2 modified by SUMO-2/3 promotes gastric cancer progression and regulates mRNA m5C methylation. Cell Death Dis 12: 842, 2021.
27. Mei L, Shen C, Miao R, Wang JZ, Cao MD, Zhang YS, Shi LH, Zhao GH, Wang MH, Wu LS and Wei JF: RNA methyltransferase NSUN2 promotes gastric cancer cell proliferation by repressing p57Kip2 by an m5C-dependent manner. Cell Death Dis 11: 270, 2020.
28. Yang R, Liang X, Wang H, Guo M, Shen H, Shi Y, Liu Q, Sun Y, Yang L and Zhan M: The RNA methyltransferase NSUN6 suppresses pancreatic cancer development by regulating cell proliferation. Ebiomedicine 63: 103195, 2021.
29. Awah CU, Winter J, Mazdoom CM and Ogunwobi OO: NSUN6, an RNA methyltransferase of 5-mC controls glioblastoma response to temozolomide (TMZ) via NELFB and RPS6KB2 interaction. Cancer Biol Ther 22: 587-597, 2021.
30. Blaze J, Navickas A, Phillips HL, Heissel S, Plaza-Jennings A, Miglani S, Asgharian H, Foo M, Katanski CD, Watkins CP, et al: Neuronal Nsun2 deficiency produces tRNA epitranscriptomic alterations and proteomic shifts impacting synaptic signaling and behavior. Nat Commun 12: 4913, 2021.
31. Lu L, Zhu G, Zeng H, Xu Q and Holzmann K: High tRNA Transferase NSUN2 Gene expression is associated with poor prognosis in head and neck squamous carcinoma. Cancer Invest 36: 246-253, 2018.
32. Haag S, Warda AS, Kretschmer J, Gunnigmann MA, Hobartner C and Bohnsack MT: NSUN6 is a human RNA methyltransferase that catalyzes formation of m5C72 in specific tRNAs. RNA 21: 1532-1543, 2015.
33. Zhou L, Yang C, Zhang N, Zhang X, Zhao T and Yu J: Silencing METTL3 inhibits the proliferation and invasion of osteosarcoma by regulating ATAD2. Biomed Pharmacother 125: 109964, 2020.
34. Zhou X, Yang Y, Li Y, Liang G, Kang D, Zhou B and Li Q: METTL3 contributes to osteosarcoma progression by increasing DANCR mRNA stability via m6A modification. Front Cell Dev Biol 9: 784719, 2021.
35. Jiang R, Dai Z, Wu J, Ji S, Sun Y and Yang W: METTL3 stabilizes HDAC5 mRNA in an m6A-dependent manner to facilitate malignant proliferation of osteosarcoma cells. Cell Death Discov 8: 179, 2022.
36. Yang M, Wei R, Zhang S, Hu S, Liang X, Yang Z, Zhang C, Zhang Y, Cai L and Xie Y: NSUN2 promotes osteosarcoma progression by enhancing the stability of FABP5 mRNA via m5C methylation. Cell Death Dis 14: 125, 2023.
37. Yang J, Tang J, Li J, Cen Y, Chen J and Dai G: Effect of activation of the Akt/mTOR signaling pathway by EEF1A2 on the biological behavior of osteosarcoma. Ann Transl Med 9: 158, 2021.
38. Livak KJ and Schmittgen TD: Analysis of relative gene expression data using real-time quantitative PCR and the 2(-Delta Delta C(T)) Method. Methods 25: 402-408, 2001.
39. Selmi T, Hussain S, Dietmann S, Heiß M, Borland K, Flad S, Carter JM, Dennison R, Huang YL, Kellner S, et al: Sequence- and structure-specific cytosine-5 mRNA methylation by NSUN6. Nucleic Acids Res 49: 1006-1022, 2021.

40. Wu S, Zhang S, Wu X and Zhou X: m⁶A RNA methylation in cardiovascular diseases. Mol Ther 28: 2111-2119, 2020.

41. Shen H, Lan Y, Zhao Y, Shi Y, Jin J and Xie W: The emerging roles of N6-methyladenosine RNA methylation in human cancers. Biomark Res 8: 24, 2020.

42. Wang S, Sun C, Li J, Zhang E, Ma Z, Xu W, Li H, Qiu M, Xu Y, Xia W, *et al*: Roles of RNA methylation by means of N⁶-methyladenosine (m⁶A) in human cancers. Cancer Lett 408: 112-120, 2017.

43. Shinoda S, Kitagawa S, Nakagawa S, Wei FY, Tomizawa K, Araki K, Araki M, Suzuki T and Suzuki T: Mammalian NSUN2 introduces 5-methylcytidines into mitochondrial tRNAs. Nucleic Acids Res 47: 8734-8745, 2019.

44. Auxilien S, Guerineau V, Szweykowska-Kulinska Z and Golinelli-Pimpaneau B: The human tRNA m (5) C methyl-transferase Misu is multisite-specific. RNA Biol 9: 1331-1338, 2012.

45. Hussain S: The emerging roles of cytosine-5 methylation in mRNAs. Trends Genet 37: 498-500, 2021.

46. Xu X, Zhang Y, Zhang J and Zhang X: NSUN2 promotes cell migration through methylating autotaxin mRNA. J Biol Chem 295: 18134-18147, 2020.

47. Su J, Wu G, Ye Y, Zhang J, Zeng L, Huang X, Zheng Y, Bai R, Zhuang L, Li M, *et al*: NSUN2-mediated RNA 5-methylcytosine promotes esophageal squamous cell carcinoma progression via LIN28B-dependent GRB2 mRNA stabilization. Oncogene 40: 5814-5828, 2021.

48. Jia L, Ge X, Du C, Chen L, Zhou Y, Xiong W, Xiang J, Li G, Xiao G, Fang L and Li Z: EEF1A2 interacts with HSP90AB1 to promote lung adenocarcinoma metastasis via enhancing TGF-β/SMAD signalling. Br J Cancer 124: 1301-1311, 2021.

49. Losada A, Munoz-Alonso MJ, Martinez-Diez M, Gago F, Dominguez JM, Martinez-Leal JF and Galmarini CM: Binding of eEF1A2 to the RNA-dependent protein kinase PKR modulates its activity and promotes tumour cell survival. Br J Cancer 119: 1410-1420, 2018.

50. Sun Y, Du C, Wang B, Zhang Y, Liu X and Ren G: Up-regulation of eEF1A2 promotes proliferation and inhibits apoptosis in prostate cancer. Biochem Biophys Res Commun 450: 1-6, 2014.

51. Lee MH, Choi BY, Cho YY, Lee SY, Huang Z, Kundu JK, Kim MO, Kim DJ, Bode AM, Surh YJ, *et al*: Tumor suppressor p16 (INK4a) inhibits cancer cell growth by downregulating eEF1A2 through a direct interaction. J Cell Sci 126: 1744-1752, 2013.